




Vertebrate population trends are influenced by interactions between land use, climatic position, habitat loss and climate change

Jessica J. Williams¹  | Robin Freeman² | Fiona Spooner³  | Tim Newbold¹ 

¹Centre for Biodiversity and Environment Research, Department of Genetics, Evolution and Environment, University College London, London, UK

²Institute of Zoology, Zoological Society of London, London, UK

³Our World in Data at the Global Change Data Lab, Oxford, UK

Correspondence

Jessica J. Williams, Centre for Biodiversity and Environment Research, Department of Genetics, Evolution and Environment, University College London, London, UK. Email: jessica.williams.16@ucl.ac.uk

Funding information

Royal Society, Grant/Award Number: IE161031, RG160501 and UF150526

Abstract

Rapid human-driven environmental changes are impacting animal populations around the world. Currently, land-use and climate change are two of the biggest pressures facing biodiversity. However, studies investigating the impacts of these pressures on population trends often do not consider potential interactions between climate and land-use change. Further, a population's climatic position (how close the ambient temperature and precipitation conditions are to the species' climatic tolerance limits) is known to influence responses to climate change but has yet to be investigated with regard to its influence on land-use change responses over time. Consequently, important variations across species' ranges in responses to environmental changes may be being overlooked. Here, we combine data from the Living Planet and BioTIME databases to carry out a global analysis exploring the impacts of land use, habitat loss, climatic position, climate change and the interactions between these variables, on vertebrate population trends. By bringing these datasets together, we analyse over 7,000 populations across 42 countries. We find that land-use change is interacting with climate change and a population's climatic position to influence rates of population change. Moreover, features of a population's local landscape (such as surrounding land cover) play important roles in these interactions. For example, populations in agricultural land uses where maximum temperatures were closer to their hot thermal limit, declined at faster rates when there had also been rapid losses in surrounding semi-natural habitat. The complex interactions between these variables on populations highlight the importance of taking intraspecific variation and interactions between local and global pressures into account. Understanding how drivers of change are interacting and impacting populations, and how this varies spatially, is critical if we are to identify populations at risk, predict species' responses to future environmental changes and produce suitable conservation strategies.

KEYWORDS

biodiversity, BioTIME, global, land-use change, Living Planet database, population trends, precipitation, temperature, time-series, vertebrates

1 | INTRODUCTION

Global animal populations are facing rapid human-driven environmental changes (IPBES, 2019). According to the Living Planet Index (LPI), average vertebrate population abundance has fallen by two-thirds in the last 50 years (WWF, 2020), with declines being clustered in certain locations around the world (Leung et al., 2020). However, studies of different time-series data, such as the BioTIME database, report little change in abundance over time for the majority of populations (Dornelas et al., 2019). Many reasons have been put forward as to why the conclusions drawn regarding global populations trends differ between the datasets, including selection biases, publication biases, monitoring methods (population- or assemblage-level), extreme clusters within the datasets and geographic biases (Dornelas et al., 2019; Gonzalez et al., 2016; Leung et al., 2020). Whatever the overall trend, we need to understand the drivers underlying population fluctuations. Furthering our understanding as to why, and which, populations are changing or staying constant may help us to identify why we see such differences in trends between time-series datasets.

Recent studies investigating the influence of drivers of change on biodiversity have primarily focused on the impacts of climate and land-use change (Antão et al., 2020; Daskalova et al., 2020; Northrup et al., 2019; Spooner et al., 2018). Using BioTIME assemblage time-series data, Antão et al. (2020) found that the abundance trends of temperate terrestrial biodiversity were not coupled to temperature changes. However, this study did not account for land-use changes, and changes in forest cover have been found to impact population changes, with both declines and increases observed to intensify after forest loss (Daskalova et al., 2020). Neither of these studies accounted for interactions between land-use change and climate change. Drivers of change are not occurring in isolation, and as such interactions between land-use and climate change are critical to take into account when studying how populations are changing (Mantyka-Pringle et al., 2012; Oliver & Morecroft, 2014; Sirami et al., 2017; Williams & Newbold, 2020). Indeed, when interactions are accounted for, a different picture is drawn as to the influence of global drivers on populations. For example, a global-level analysis using the Living Planet database (LPD) not only found that declines in endothermic vertebrate populations were greater at sites where there had been rapid increases in temperature, but also, for mammals, that this effect interacted with land-use change, with declines due to rapid warming amplified in areas with high rates of conversion from natural to agricultural land uses (Spooner et al., 2018). Interestingly though, unlike forest loss (Daskalova et al., 2020), land-use change on its own did not influence population changes (Spooner et al., 2018). At a more local scale, climatic changes (warming and drying) have also been found to interact synergistically with forest loss to influence bird declines in the northwest forests of the United States (Northrup et al., 2019).

One route by which land-use change and climate change could interact to impact how vertebrate populations respond to global drivers of change is through the local-scale climatic changes that

occur due to land-use change (De Frenne et al., 2019; Frishkoff et al., 2016; Williams et al., 2020; Williams & Newbold, 2020). Human-altered land uses (such as agricultural and urban areas) are, on average, hotter and drier than natural habitats (De Frenne et al., 2019; Frishkoff et al., 2016). In addition, the removal of canopy layers, such as through conversion from forest to croplands, leads to greater temperature extremes (De Frenne et al., 2019; Senior et al., 2017). For example, the average maximum daily temperatures in pastures and pineapple farms have been recorded to be around 6°C and 9°C higher than that in forests (Nowakowski et al., 2017). These local climatic differences between land uses have been associated with community shifts: At both local and global levels, human-altered land uses have been observed to favour species that can tolerate greater hot and cold extremes of temperature, and greater wet and dry extremes of precipitation (Frishkoff et al., 2015; Nowakowski et al., 2017; Waldock et al., 2020; Williams et al., 2020). As these local-scale climatic changes are occurring alongside global climatic changes, this has the potential to lead to complex interactions (Williams & Newbold, 2020).

Populations, however, do not respond to environmental changes uniformly across their species' ranges (Orme et al., 2019; Soroye et al., 2020; Spooner et al., 2018). Recent analyses are highlighting that ambient climate and, more specifically, how close the local temperature and precipitation conditions are to a species' climatic tolerance limits (climatic position), may impact how populations respond to land-use change, leading to variation in responses across species' ranges (Srinivasan et al., 2019; Williams & Newbold, 2021). At a regional level, across the Himalayas, bird species common to locations across the region were more forest-dependent (using agricultural sites less) in relatively aseasonal compared to highly seasonal locations (Srinivasan et al., 2019). At a global level, populations in environments where extreme temperatures were closer to their hot or cold thermal limits were filtered out of human-altered land uses (Williams & Newbold, 2021). Further, despite human-altered land uses being drier on average (Frishkoff et al., 2016), populations experiencing precipitation levels close to their dry tolerance limits had similar abundances in human-altered land uses and natural habitats (Williams & Newbold, 2021). In comparison, populations with a larger buffer between their dry limit and the location's minimum precipitation levels did worse (had lower abundances relative to that in natural habitat; Williams & Newbold, 2021). This variation across species' ranges has been suggested to be due, at least in part, to the local climatic changes following land-use change (Williams & Newbold, 2021). However, climatic position and its interaction with land-use have yet to be considered when analysing global population trends.

Here, we combine time-series data from the LPD and BioTIME database, with the aim to investigate whether changes in vertebrate population abundances are influenced by their climatic position, the habitat they are found within, the rates of climate change and changes in surrounding land use and, importantly, interactions between these variables. Based on the fact that conversion of natural habitat to agriculture or urban areas leads to more extreme local

temperatures (De Frenne et al., 2019), that responses to land use vary across species ranges due to the population's climatic positions (Williams & Newbold, 2021), and that past work has suggested synergistic interactions between land-use and climate change (eg, Spooner et al., 2018), we make three specific hypotheses:

1. Populations experiencing maximum or minimum temperatures closer to their upper or lower thermal tolerance limits, respectively, will decrease more rapidly in human-altered land uses compared to populations in more natural habitats, particularly in areas that have experienced greater increases in surrounding human-altered land uses.
2. For those populations experiencing maximum or minimum temperatures closer to their upper or lower thermal tolerance limits, respectively, greater rates of decline will be observed in places where hot maxima and cold minima have got more extreme over time, and this will be more pronounced in human-altered land uses compared to natural habitats.
3. Populations experiencing rapid increases in surrounding human-altered land uses as well as hotter maximum or colder minimum temperatures over time will decrease at a faster rate compared to populations not facing such changes or not experiencing these changes in tandem, particularly in human-altered land uses.

We also look at a population's climatic position with regard to their species-level precipitation limits, as precipitation affiliations have been found to have an important impact on responses to land-use change (Frishkoff et al., 2016; Williams et al., 2020). However, we do not have clear predictions regarding how populations over time will be influenced by their minimum and maximum precipitation position, due to previous mixed results and the complex effects of land use on moisture availability (Williams & Newbold, 2020). Previous work found that species from areas with lower mean annual precipitation (ie, dry-affiliated species) were more likely to persist within agricultural areas compared to those from areas with, on average, wetter climates (Frishkoff et al., 2016). Yet, other studies focusing on extreme precipitation conditions have reported shifts towards a higher proportion of species affiliated with greater extremes of precipitation (both drier and wetter) in communities in human-altered land uses compared to natural habitats (Williams et al., 2020). Species also alter their use of natural versus human-altered land uses across precipitation gradients (Frishkoff et al., 2016). For example, relative to populations in more natural habitats, tropical populations in plantations and croplands experiencing minimum precipitation levels further from their dry tolerance limit had lower abundances than populations experiencing minimum precipitation levels closer to their dry limit (Williams & Newbold, 2021). Further, populations experiencing precipitation levels closer to species' wet tolerance limit have been found to have a lower probability of occurrence in human-altered land uses relative to that in natural habitats (Williams & Newbold, 2021). However, the biological mechanisms underlying these results are unclear. On top of this, habitat conversion and the ongoing drying trends in certain parts of the world, such as the

tropics (Lau & Kim, 2015), are favouring the same, dry-affiliated species (Frishkoff et al., 2016; Karp et al., 2017), which will likely further complicate how populations' precipitation positions interact with these variables to influence population trends. Consequently, we do not make specific hypotheses as to the impact of maximum and minimum precipitation position (ie, how close the maximum and minimum precipitation levels a population experiences are to the species' wet and dry tolerance limits, respectively) on population trends.

By bringing together these two global databases and incorporating previously overlooked variables and interactions, we complete the most comprehensive analysis to date to further our understanding of how vertebrates are being influenced by environmental changes around the world, how drivers of change are interacting, and which populations may be at higher risk from human-induced changes.

2 | METHODS

2.1 | Population time-series data

We acquired population time-series data for terrestrial vertebrates from the Living Planet database (LPD; LPI database, January 2020) and the BioTIME database (Dornelas et al., 2018; see Supplementary information, Appendix 14, for the original data citations), for the period covering 1992–2015 (to match the land-cover data, see below). These two databases together contain time-series of population estimates for over 100,000 terrestrial vertebrate populations from around the globe within our timeframe. Here, we use the term 'population' to refer to a group of individuals of the same species at the same location. We focused on vertebrates due to the reasonably comprehensive data available on their distributions, which was necessary in order to estimate species' realized climatic tolerance limits (see below).

From both the LPD and BioTIME database, we extracted annual population estimates for non-migratory terrestrial vertebrate populations whose specific locations were known (so that we could assign land-use and environmental data to the site). In the BioTIME database, if there were multiple population estimates per year, we took the mean of these. We further removed any birds or mammals classed as migratory according to data obtained from BirdLife International (2018) and Gnanadesikan et al. (2017). From the BioTIME database, we also excluded studies looking at biomass, and populations that were part of treatment studies such as burning, harvesting or predator exclusion experiments. Finally, we excluded studies that were within the Arctic Circle, spanned less than 6 years, or had 5 or fewer population estimates over the time-series (following Spooner et al., 2018). This left us with a dataset comprised of 9,601 populations, consisting of 423 species (147 mammals, 224 birds, 30 reptiles and 22 amphibian species) in 1,669 locations across 48 countries.

For each population, we calculated the average logged annual rate of population change ($\overline{\lambda_y}$), following the method used by Spooner et al. (2018). In brief, we first took the log (base 10) of

each population estimate (if an estimate was zero, we instead took the log of 1% of the mean estimate from the entire time-series, including the zeros). Second, in order to impute values for missing annual population estimates, each time-series was fit with a generalized additive model (GAM), with a smoothing parameter set to half the number of population estimates in the time-series (Collen et al., 2009). Then, $\overline{\lambda}_Y$ was calculated for each time-series using the following equation:

$$\overline{\lambda}_Y = \frac{1}{Y} \sum_0^n \left(\log_{10} \left(\frac{n_y}{n_{y-1}} \right) \right) \quad (1)$$

in which n is the population estimate for year y , and Y is the number of years from the first to the last estimate for a population.

2.2 | Land-cover data

We obtained global land-cover maps from the European Space Agency Climate Change Initiative (ESA CCI; ESA Land Cover CCI project team, Defourny, 2019). These maps are available for the years 1992–2015, at a spatial resolution of 300 m and categorize land into 37 land-cover classes (Defourny et al., 2017). We grouped these land-cover classes into the broader categories of agriculture, forest, grassland, wetland, urban, and other (we did not include the water or permanent snow and ice categories, so removed populations located in these categories; Appendix 1, Table S1), closely following the groupings used by the Intergovernmental Panel on Climate Change for change detection (Defourny et al., 2017). The land-cover category that each population was located in when the population was first recorded within the 1992–2015 timescale was recorded as its starting land-use type (there were not enough populations starting in urban or wetland land-use types to include in the analysis, so the populations in these categories were removed, leaving forest, grassland, agriculture, and other as starting land-use types).

To calculate the rate of change in land cover each population experienced over time, we first extracted the percentage of semi-natural habitat (SNH) within a 1-km radius of the population's location for each year between its first and last estimate. A radius of 1 km has previously been used when assessing the impact of land-use change on local biodiversity (Le Provost et al., 2020), and due to our focus on the *local* climatic changes brought about by land-use change, we felt that concentrating on the changes in SNH within a 1-km radius surrounding a population was appropriate (however, to check the sensitivity of our results, we also calculated the percentage change in SNH within a 5-, 10- and 50-km radius). Land-cover categories included as SNH were forest, grassland, wetland, and shrubland (Appendix 1, Table S1). We also incorporated a weighting system, in which we used the maximum percentage cover of a specific land-use (detailed in the ESA's land-use categories) to weight each category. For example, the category 'Tree cover, broadleaved, deciduous, closed to open

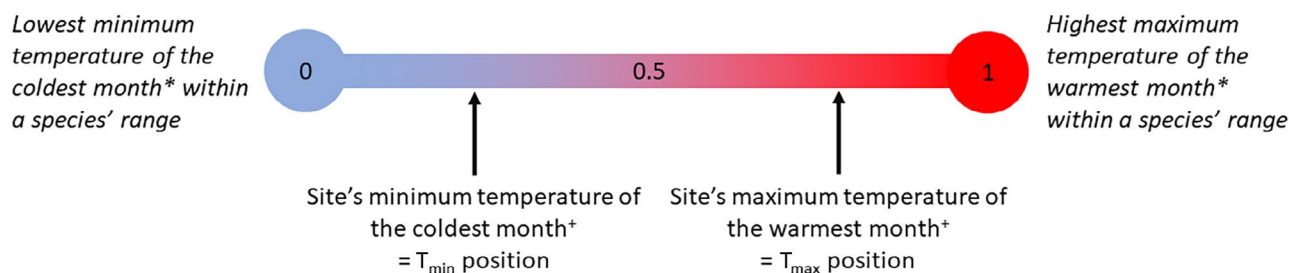
(>15%)' was given a weighting of 1, as it could cover 100% of the 300 × 300-m area, whereas the category 'Tree cover, broadleaved, deciduous, open (15–40%)' was given a weighting of 0.4, as this could cover a maximum of 40% of the 300 × 300 m (see Appendix 1, Table S1 for a full listing of the weightings; non-SNH categories were given a weighting of 0). Then, for each location with a population time-series, a linear regression was fit to the percentage of SNH within the surrounding 1-km radius over the length of the population time-series, with the resulting slope extracted to give the average annual rate of change in SNH.

2.3 | Climatic tolerance limits

We estimated species' realized climatic tolerance limits, that is, the maximum and minimum temperature and monthly precipitation that a species' experiences across its geographic distribution. We obtained expert-informed species distribution maps (extent of occurrence maps) from BirdLife International (2012) and the International Union for Conservation of Nature (IUCN, 2016a, 2016b, 2017a, 2017b, 2017c, 2018a, 2018b, 2019a, 2019b, 2019c). For each species, we extracted their native historical ranges (where they were resident, present during breeding or non-breeding seasons) and areas the species had been introduced or reintroduced (ie, excluding areas where the presence or seasonal occurrence is uncertain, species are possibly extant or vagrant, or areas classed as passages, such as areas used for short periods of time during migration). Breeding and non-breeding areas were included within species' native historical ranges because, despite being non-migratory, parts of some species' ranges were classified as, for example, extant (non-breeding). These extracted areas were then rasterized into 500 × 500-m equal-area grids (Behrmann projection). We chose this resolution so that we could include as many species as possible with very narrow ranges. Areas outside of species' elevation limits, if known (BirdLife International, 2018; IUCN, 2016a, 2016b, 2017a, 2017b, 2017c, 2018a, 2018b, 2019a, 2019b, 2019c), were removed from their distribution maps.

We obtained climate maps for the average monthly maximum temperature of the warmest month, average monthly minimum temperature of the coldest month, and precipitation of the wettest and driest months from WorldClim Version 1.4 (Hijmans et al., 2005). These maps had a resolution of 30 arc seconds and encompassed averaged yearly values from 1960 to 1990. We resampled these climate maps using bilinear interpolation to 500 × 500-m equal-area grids (Behrmann projection) to match the projection of the species' distribution maps. We overlaid the species' distribution map on these four climatic variables and extracted the highest maximum temperature of the warmest month and precipitation of the wettest month, and the lowest minimum temperature of the coldest month and precipitation of the driest month across each species' distribution (ArcGIS 10.4). These values provided our estimates of each species' realized upper and lower temperature and precipitation tolerance limits (Figure 1).

Thermal tolerance limits



Precipitation tolerance limits

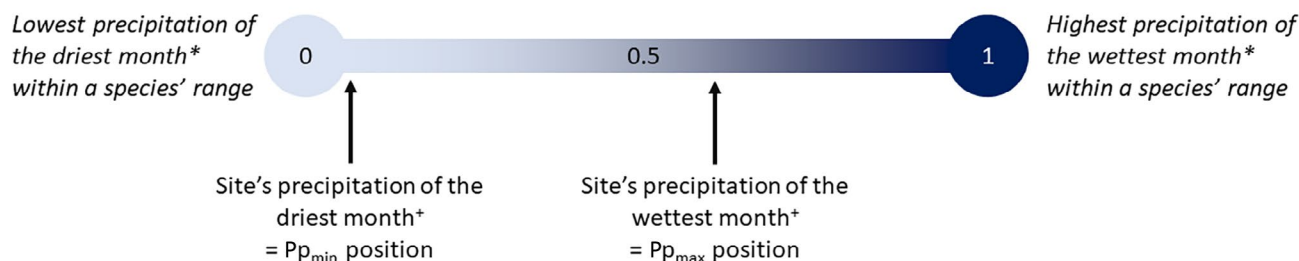


FIGURE 1 A visual example of how the starting climatic positions (T_{\max} , T_{\min} , Pp_{\max} and Pp_{\min} position) were calculated for each population. 0 and 1 represent the species-level realized minimum and maximum, respectively, thermal or precipitation tolerance limits, extracted from species' distribution maps overlaid on climatic data from WorldClim Version 1.4 (denoted by the *; Hijmans et al., 2005). The starting climatic positions were calculated by standardizing the population's site-level temperature and precipitation data (obtained from the Climatic Research Unit, denoted by +; Harris & Jones, 2020) in the year that the population was first recorded to range between 0 and 1 relative to the species-level climatic tolerance limits. For example, a T_{\max} position closer to 1 means that the maximum temperature of the warmest month experienced by a population was closer to the highest maximum temperature of the warmest month across the species' range. Similarly, a Pp_{\min} position closer to 0 describes a population that experienced precipitation levels in their driest month that were closer to the lowest precipitation of the driest month across the species' range. This figure is adapted from Williams and Newbold (2021) [Colour figure can be viewed at [wileyonlinelibrary.com](https://onlinelibrary.wiley.com)]

2.4 | Climate change and starting climatic position

Monthly average daily maximum and minimum temperature, and monthly precipitation data were acquired from the gridded ($0.5^\circ \times 0.5^\circ$) Climatic Research Unit (CRU) Time-series data v. 4.03 (Harris & Jones, 2020). From these, we found the highest monthly average daily maximum temperature, lowest monthly average daily minimum temperature, and maximum (wettest) and minimum (driest) monthly precipitation per year at the location of each observed population within our dataset. For each population, values for the four climatic variables were extracted for each year between the first and last population estimate. Linear regressions were fit to each set of climatic variables for each population, with the slopes of these extracted to give the average annual rate of change in maximum temperature of the warmest month, minimum temperature of the coldest month and precipitation of the wettest and driest months over the length of the population time-series.

For each population, we calculated their starting climatic position with regard to the maximum temperature of the warmest month (T_{\max} position), minimum temperature of the coldest month (T_{\min} position), precipitation of the wettest month (Pp_{\max} position) and precipitation of the driest month (Pp_{\min} position). These positions describe the thermal and precipitation conditions (CRU Time-series data v. 4.03; Harris

& Jones, 2020) a population experienced in the first year they were measured at a site, standardized to range between 0 and 1 relative to the lower and upper realized temperature or precipitation tolerance limits of the species (where, for thermal tolerance limits, 0 = minimum realized temperature tolerance limit and 1 = maximum realized temperature tolerance limit and for precipitation tolerance limits, 0 = minimum (dry) realized precipitation tolerance limit and 1 = maximum (wet) realized precipitation tolerance limit; Figure 1). We chose to use the temperature and precipitation conditions a population experienced in the first year of their time-series because we wanted a measure of where each population started in relation to their species-level climatic limits. However, to check the sensitivity of our results, we also calculated starting climatic position using the average maximum and minimum temperature and precipitation conditions (CRU Time-series data v. 4.03; Harris & Jones, 2020) in the three years up to and including the first year of a population's time-series and ran a model (see below) using this measure (Appendix 4).

2.5 | Distance to range edge

Within our analyses, we also accounted for a population's location relative to their species' range edge. For each population in our

dataset, we found the shortest distance from their location to their species' range edge and, to account for range size, divided it by the greatest distance a population of that species could be from their range edge (calculated by transforming species distribution maps into spatial points dataframes). Therefore, each population had a standardized (between 0 and 1) distance to range edge measure, where a value of 0 meant the population was located at the species' range edge, and values closer to 1 meant the population was closer to the range centre. Populations that were recorded outside of their distributions as stated by the distribution maps (BirdLife International, 2012; IUCN, 2016a, 2016b, 2017a, 2017b, 2017c, 2018a, 2018b, 2019a, 2019b, 2019c), were removed.

The final dataset comprised of 7,123 populations, consisting of 341 species (126 mammals, 186 birds, 12 reptiles and 17 amphibian species) in 1,151 locations across 42 countries (Appendix 2, Figure S1; the final dataset is available in a figshare repository, Williams et al., 2021; <https://doi.org/10.6084/m9.figshare.16895851>).

2.6 | Statistical analyses

We used linear mixed-effects models to investigate how the rate of population change was affected by land-use type and change, the population's climatic position and the rate of climate change experienced. We constructed 42 candidate models, with the average logged annual rate of population change ($\bar{\lambda}_y$) as the response variable (see Appendix 3, Tables S2–S3, for information on the choice of candidate models). The 'full' model included all of the following variables and interactions, with the other 41 candidate models including a subset, based on our hypotheses and the aims of this study. Fixed effects included: (a) the population's starting land-use type, (b) the rate of change in SNH the population experienced, (c) their starting T_{\max} , T_{\min} , Pp_{\max} and Pp_{\min} positions and (d) the rate of change in climate experienced (for the four climatic variables detailed above; Table 1; correlations between continuous variables were checked, Appendix 3, Table S4). Following our hypotheses, three 3-way interactions were considered: (a) starting land-use type \times rate of change in SNH \times starting climatic position, to look at whether populations in human-altered land uses experiencing temperatures and precipitation closer to their climatic limits as well as greater rates of decreases in SNH have larger negative rates of population change, (b) starting land-use type \times starting climatic position \times rate of change in climate (with the same focal climatic variable as the climatic position, for example, starting land-use type \times starting T_{\max} position \times rate of change in maximum temperature of the warmest month), to explore whether populations in human-altered land uses experiencing temperatures and precipitation closer to their climatic limits on top of greater increases in climatic extremes have larger negative rates of population change and (c) starting land-use type \times rate of change in SNH \times rate of change in climate, to look at whether populations in human-altered land uses experiencing greater decreases in SNH as well as increases in extreme climatic conditions have larger negative rates of population

change. Any lower-order two-way interactions between the variables in each three-way interaction were also included (Table 1, Table S2). Covariates included the distance of a population from its species' range edge, and its interaction with starting land-use type and with the rate of change in SNH (as well as the three-way interaction between these variables), to account for potential response or behavioural differences due to proximity to range edge (Liebl & Martin, 2012; Orme et al., 2019). In all models, we included four random intercept terms: species name, vertebrate class, study site and database (LPD or BioTIME; Table 1). We compared candidate models using AIC values and Akaike weights (using the MuMIn package v.1.43.17 in R 3.6.0; Barton, 2020; R Core Team, 2019). From the selection of candidate models, the full model (which included all of the considered terms) received overwhelming support (Akaike weight ≈ 1 ; Appendix 3, Table S3). We, henceforth, present the results from this 'final model'. We ensured our model was not overfitted by splitting the final model (a) per each three-way interaction (and then including the lower-order interactions and main effects included) and (b) per each climatic variable (ie, running a model in which the only climatic variables considered were those including the maximum temperature of the warmest month, minimum temperature of the coldest month, precipitation of the wettest month or precipitation of the driest month) and then checking to see if the resulting effects were similar to those produced by the final model. All of the above was completed in ArcGIS 10.4 (ESRI 2015) and R 3.6.0 (R Core Team, 2019) using packages dplyr v.0.8.3 (Wickham et al., 2019), lme4 v.1.1.26 (Bates et al., 2015), MuMIn v.1.43.17 (Barton, 2020), ncdf4 v.1.17 (Pierce, 2019), plyr v.1.8.6 (Wickham, 2011), raster v.2.8–19 (Hijmans, 2019) and tidyr v.1.0.0 (Wickham & Henry, 2019).

2.7 | Sensitivity tests

We compared the ESA land cover maps to recently produced global maps of terrestrial habitat types (Jung et al., 2020), to check the consistency of land-use types across data sources. These latter maps are only available for 2015–2019, so for each site in our final dataset ($n = 1,151$), we compared the land-use types between the 2015 ESA land cover map and Jung et al.'s (2020) global map of terrestrial habitat types for 2015. In particular, we wanted to ensure that there were not a large number of plantations or pastures at sites that we classed as forest or grasslands, respectively, as land-cover maps may miss these land uses.

The IUCN and BirdLife International species' distribution maps (BirdLife International, 2012; IUCN, 2016a, 2016b, 2017a, 2017b, 2017c, 2018a, 2018b, 2019a, 2019b, 2019c) provide data for a wide range of vertebrates from around the world, and as such have been used extensively (Allan et al., 2019; Herkt et al., 2017; Khaliq et al., 2017; Shackelford et al., 2015). However, they do contain inaccuracies as they tend to overestimate the area of occupancy and underestimate species' extent-of-occurrence (Herkt et al., 2017; Hurlbert & Jetz, 2007). Therefore, to check the robustness of our

TABLE 1 Parameters included in the final model. Symbols represent variables within the same two- or three-way interaction (for example, starting land-use type and rate of change in semi-natural habitat both have a ♦ symbol, indicating that we included a two-way interaction between these variables – starting land-use type × rate of change in semi-natural habitat – in the final model). Interactions combining both starting climatic position and rate of change in climate included the same climatic variable (eg, starting T_{\max} position × rate of change in maximum temperature of the warmest month, or starting P_{\min} position × rate of change in precipitation of the driest month). Interactions between starting positions with respect to different climate variables, or between rates of change in different climatic variables were not included

Parameter	Description	Type of effect	Included in an interaction?	
			2-way	3-way
Starting land-use type	The land-use type (forest, grassland, agriculture, or other) the population was within in the first year of its time-series	Fixed, categorical	♦ ♠ ≡ ⊂	∞ ⊗ * ⇔
Rate of change in semi-natural habitat	The average annual rate of change in the percentage of semi-natural habitat (which included forest, grassland, wetland and shrubland) within a 1-km radius of the population, over the length of the population time-series	Fixed, continuous, quadratic	♦ ♠ ⊕ ∇	∞ ⊗ ⇔
Starting climatic position	The a. maximum temperature of the warmest month (T_{\max}), b. minimum temperature of the coldest month (T_{\min}), c. precipitation of the wettest month (P_{\max}), and d. precipitation of the driest month (P_{\min}), a population experienced in the first year they were measured, relative to the species-level upper and lower realized thermal (for a and b) or precipitation (for c and d) tolerance limits	Fixed, continuous, quadratic	♠ ♠ §	∞ *
Rate of change in climate	The average annual rate of change in a. maximum temperature of the warmest month, b. minimum temperature of the coldest month, c. precipitation of the wettest month, and d. precipitation of the driest month, over the length of the population time-series	Fixed, continuous, quadratic	≡ ⊕ §	⊗ *
Distance to range edge	The distance of a population from their species' geographic range edge, standardized to account for overall range size	Fixed, continuous, linear	⊂ ∇	⇔
Species name	Species binomial, to account for interspecific differences in responses.	Random intercept		
Class	The vertebrate Class (Mammalia, Aves, Reptilia or Amphibia), to account for broad taxonomic differences in population trends	Random intercept		
Study site	ID based on the population's location (latitude and longitude), included to account for site-specific effects	Random intercept		
Database	The database the population's time-series data were acquired from (Living Planet database or BioTIME database), to account for differences between the databases (differences in inclusion criteria or sampling method, for example)	Random intercept		

climatic position measure, we also calculated species' climatic limits using occurrence records from the Global Biodiversity Information Facility (GBIF; GBIF.org, 2015), rather than species' distribution maps (Appendix 4). Further, to ensure that our climatic position measure was robust to the climatic data used to estimate climatic limits, we calculated another estimate of a population's climatic position, this time using the CRU Time-series data v. 4.03 (Harris & Jones, 2020), extracting temperature and precipitation data from 1992, to calculate species' climatic limits (rather than using WorldClim data). Additionally, we calculated a fourth estimate of climatic limits, using both GBIF occurrence records (rather than species' distribution maps) and CRU Time-series data (rather than WorldClim data). We compared both the resulting climatic positions themselves and the results of models run (with the same structure as the final model)

using the climatic positions calculated through these different methods of estimating climatic limits (Appendix 4).

Further, using the same structure as the final model, we also ran models that (a) included the average annual rate of change in the percentage of forest (instead of SNH) within a 1-km radius of the population's location (calculated in the same way as for SNH, but only including the forest category; Appendix 1, Table S1), to investigate whether it was change in forest specifically, rather than semi-natural habitat, driving differences in population trends (Daskalova et al., 2020); (b) included percentage of SNH within a 1-km radius of the population in the first year they were recorded, rather than starting land-use type, to see if this explained more variance in the data (Appendix 5); (c) only included time-series with $R^2 \geq 0.5$ when fit to the GAM, to remove populations with more

variable estimates over the years, for which interpolated values may not be as accurate (Appendix 8); (d) excluded time-series with $\bar{\lambda}_Y$ above and below the upper and lower 97.5th and 2.5th percentile, respectively, to ensure results were not being influenced by extreme positive or negative rates of population change (we do not remove extreme values in our final model, following Daskalova et al., (2020) and Spooner et al., (2018); Appendix 9); (e) excluded populations from the genus *Gyps*, as a previous study using the LPD found that they had a big influence on model estimates (Green et al., 2020; Appendix 10); and (f) excluded ectotherms, to check these taxa were not driving any observed declines (Appendix 11). Further, to ensure that removing populations outside of their species' ranges did not affect our results, we ran two more models (with the same structure as the final model but excluding all terms containing distance to range edge), one including and one excluding populations beyond their species ranges as stated by BirdLife International (2012) and IUCN (2016a, 2016b, 2017a, 2017b, 2017c, 2018a, 2018b, 2019a, 2019b, 2019c; Appendix 12). We also carried out cross-validation tests to ensure there were no overly influential locations or species in our dataset (Appendix 13). We checked to see if we could run models separately for each vertebrate class (Mammalia, Aves, Reptilia and Amphibia), but there were insufficient data.

3 | RESULTS

The 7,123 populations analysed had an average time-series length of 15 years, covered a variety of starting land-use types and climatic positions and, across these populations, there were both increases and decreases experienced in surrounding SNH and all climatic variables (Table 2).

In summary, our results highlight the complexity of the impact that climatic position, land-use type and change, and climate change have on populations over time, with all these variables interacting with each another in complex ways (see Appendix 3, Table S5 for the fixed-effects included in the final model, and Table S6 for more details on the continuous variables). Notably, the rate of change in SNH surrounding a population affected the rate of population change, with this differing slightly depending on a population's starting land-use type: For populations starting in the forest, the average annual rate of population change was relatively consistent across different rates of change in surrounding SNH (although it decreased slightly under rapid increases and decreases in surrounding SNH), whereas in grassland and agriculture, rates of population change increased as rates of change in surrounding SNH got higher (Figure 2). In general, starting land-use type appeared to play an important role within interactions, particularly in its influence on how populations were affected by rates of change in climate and their starting climatic position. The fixed effects that were included in the final model (Appendix 3, Table S5) explained almost 5% of the variation in the rate of population change (marginal pseudo- R^2 , *sensu* Nakagawa & Schielzeth,

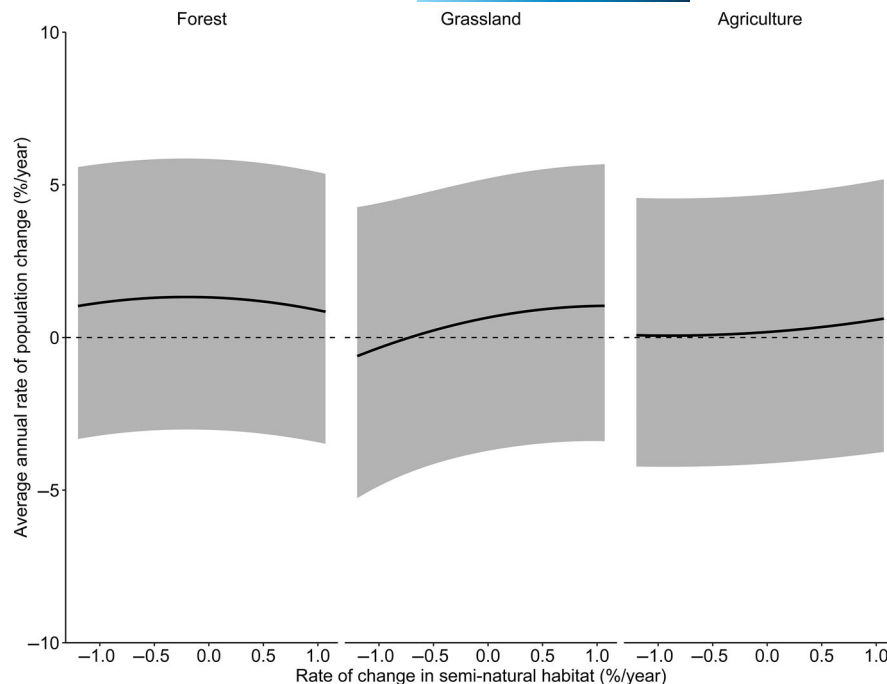
TABLE 2 Summary statistics for the population time-series analysed, split by the originating database (the Living Planet database or BioTIME database). The average annual rate of change in semi-natural habitat refers to change within a 1-km radius surrounding each population. Fitted values were based on fixed effects only

	Living Planet database	BioTIME database
Number of populations analysed	367	6756
Average annual rates of population change (% / year)		
Mean of observed (and fitted) values	-2.83 (1.09)	-0.03 (0.42)
Median of observed (and fitted) values	-0.53 (0.86)	0 (0.47)
Number of populations with positive (↑) or negative (↓) values	↑ 152 ↓ 215	↑ 3299 ↓ 3319
Mean length of population time-series (years)	13	15
Number of countries from which populations originated	42	4
Average annual rates of change in semi-natural habitat		
Range (% / year)	-7.75 to 3.97	-7.27 to 9.24
Mean (% / year)	-0.17	0.02
Median (% / year)	0	0.03
Number of populations with a positive (↑) or negative (↓) values	↑ 137 ↓ 168	↑ 3882 ↓ 2592
Percentage of populations starting in each starting land-use type (% to 1 decimal place)		
Forest	58.9	54.2
Grassland	3.5	11.6
Agriculture	17.7	28.3
Other	19.9	5.8

2013) and together with the random effects, explained 68% of the variation (conditional pseudo- R^2).

Whilst testing the sensitivity of our results, we included the percentage of SNH within a 1-km radius of the population in the first year they were measured (rather than starting land-use type); the results indicated that populations surrounded by a higher percentage of human-altered habitats at the start of recording often had greater negative rates of population change (Appendix 5, Figures S13–S16). This is another very interesting result and we present it in the Supplementary information (due to it being a post hoc test, as well as having a higher AIC value and lower marginal R^2 compared to our final model, and not capturing the difference between populations starting in forest versus grassland). Below we do not plot the results for populations that started in habitats classed as 'other' because, following our hypotheses, we want to focus on how the impact of climatic position, land-use and climate change on the rate of population change differs between those starting in human-altered habitats (agriculture) compared to those in more natural habitats

FIGURE 2 The average annual rate of population change depending on the average annual rate of change in semi-natural habitat, split by the land-use type a population was in when the first population measure was recorded. Error margins denote ± 1 standard error



(forest and grasslands). We use heat maps to display the results of each focal three-way interaction – (a) starting land-use type \times rate of change in SNH \times starting climatic position, (b) starting land-use type \times starting climatic position \times rate of change in climate and (c) starting land-use type \times rate of change in SNH \times rate of change in climate – see Figure 3 for guidance on how to interpret these heat maps. We also present a series of line graphs in the Supplementary information to provide an alternative presentation of the three-way interaction results (Appendix 3, Figures S2–S4).

We found support for our first hypothesis. With regard to T_{\max} position, populations experiencing maximum temperatures closer to their upper thermal tolerance limits (high T_{\max} position) decreased more rapidly in human-altered land uses (especially in areas that experienced greater decreases in surrounding semi-natural habitat), compared to populations in more natural habitats (Figure 4a). Interestingly, however, populations starting in agricultural land uses with lower starting T_{\max} positions (indicating they initially experienced maximum temperatures further from their hot thermal limit) also had more negative rates of population change in areas that had experienced more rapid increases in SNH in the surrounding landscape (Figure 4a). With regard to T_{\min} position, despite populations in the forest, grassland and agriculture that experienced minimum temperatures closer to their lower thermal tolerance limits (low T_{\min} position) having similar rates of population change, agricultural populations experiencing more rapid increases in surrounding SNH were increasing fastest (Figure 4b).

Support for our second and third hypotheses was mixed. Unexpectedly, and not in line with these hypotheses, populations in agricultural areas that experienced more negative rates of change in maximum temperature (ie, hot extremes got cooler over time), also often had negative rates of population change (and vice versa, with agricultural populations experiencing warmer maximum

temperatures having higher rates of population increase; Figures 5a and 6a). With regard to T_{\min} position, and in contradiction to our second hypothesis, populations in agriculture with lower starting T_{\min} positions (experiencing minimum temperatures closer to their cold thermal limit), had more positive rates of population change compared to populations with higher T_{\min} positions in areas that experienced decreases in minimum temperature (Figure 5b). However, in support of our third hypothesis, agricultural populations in areas where minimum temperatures had got colder and there had been rapid declines in surrounding SNH often had lower rates of population change (Figure 6b); although unexpectedly, under the same conditions, greater negative rates of population change were observed in grasslands (Figure 6b).

In terms of precipitation, for those populations experiencing minimum precipitation levels close to their dry tolerance limit (low Pp_{\min} position), those that started in agriculture were decreasing more rapidly (Figure 4d). Notably, we found that for populations with a low Pp_{\min} position, those also experiencing rapid decreases in minimum precipitation had negative rates of population change, the lowest of which was observed for those populations starting in agriculture (Figure 5d). A populations' starting Pp_{\max} position also interacted with the rate of change in SNH, with this effect differing between starting land-use types (Figure 4c). Effects of Pp_{\max} positions and rate of change in SNH were stronger for populations starting in grassland sites compared to forest or agriculture, with rapid declines observed for populations experiencing maximum precipitation closer to their wet tolerance limit on top of swift decreases in surrounding SNH (Figure 4c).

Further, it was interesting to observe that, across climatic positions and different rates of change in climate and surrounding SNH, the average annual rates of population change for populations starting in forested sites were relatively similar (increasing at a rate of

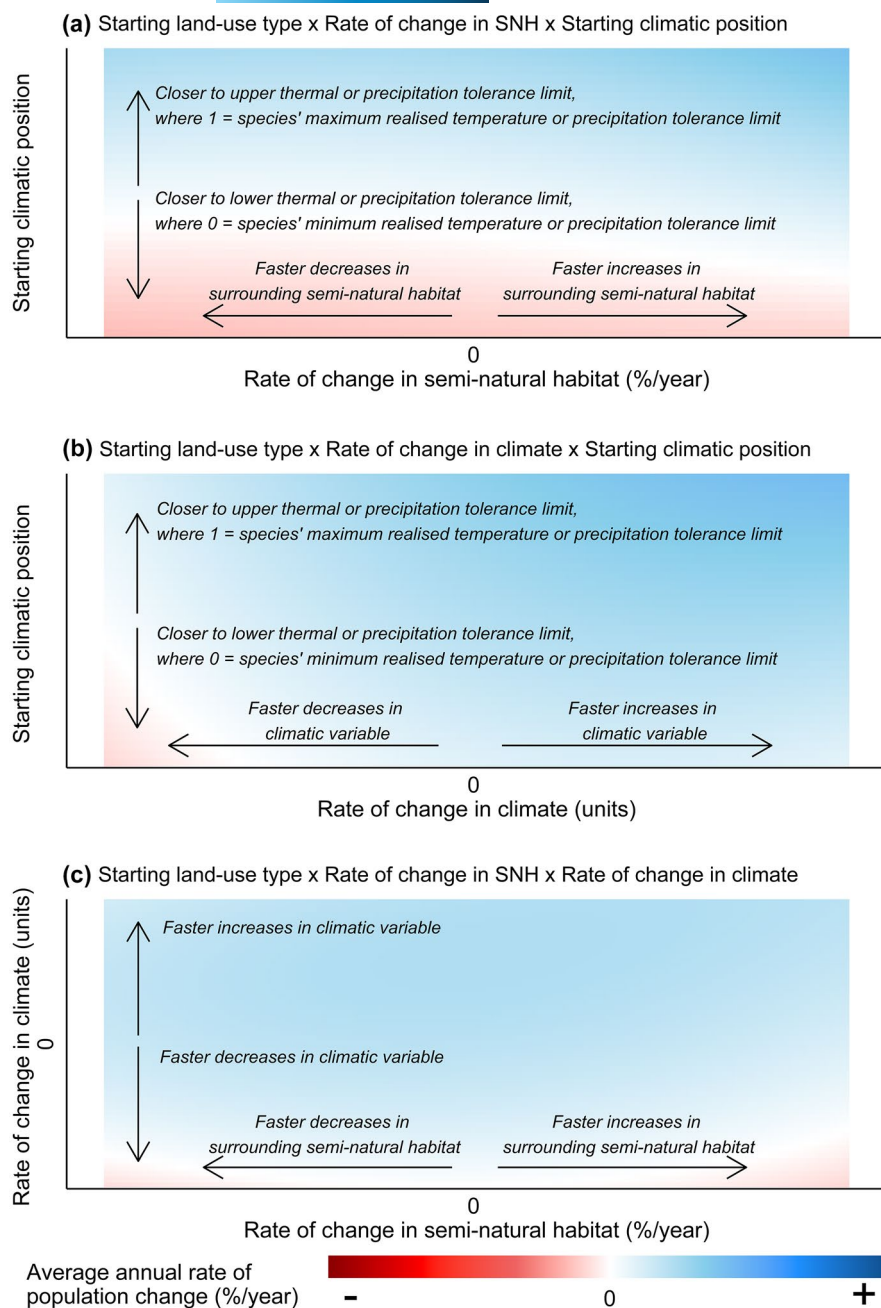


FIGURE 3 Guidance on how to interpret the heat maps used to display the modelled results for the three focal interactions – (a) starting land-use type \times rate of change in SNH \times starting climatic position (Figure 4), (b) starting land-use type \times starting climatic position \times rate of change in climate (Figure 5) and (c) starting land-use type \times rate of change in SNH \times rate of change in climate (Figure 6). The colours within the heat maps represent the average annual rate of population change (%/year). Blues represent population increases (+), and reds represent population declines (-), with darker colours representing faster rates of change in both directions. The figures below also display contour lines (and labels), indicating conditions that share the same rates of population change. The panels in the figures below are also split into the starting land-use type (forest, grassland, and agriculture), which is indicated at the top of each column [Colour figure can be viewed at [wileyonlinelibrary.com](https://onlinelibrary.wiley.com/doi/10.1111/gcb.15978)]

around 1%). Conversely, often the most variation in the rate of population change was observed for populations that started in grasslands (Figures 4–6).

3.1 | Sensitivity tests

Land-use types extracted from the 2015 ESA land cover map (ESA Land Cover CCI project team, Defourny, 2019) and the 2015 global map of terrestrial habitat types (Jung et al., 2020) were the same for over 70% of sites in our dataset (Appendix 6, Table S8 and S9). Out of the sites that differed, there were a low number of discrepancies between forest and plantation ($n = 24$, 2.1% of all sites in the

dataset) and between grassland and pasturelands ($n = 6$, 0.5% of all sites in the dataset).

Using the average temperature and precipitation conditions in the three years up to and including the first year of a population's time-series to calculate the climatic position (rather than the temperature and precipitation in the first year) explained almost the same proportion of variation in the rate of population change but the model had a higher AIC ($\Delta AIC = 25.9$). Overall, the model produced very similar results to those presented above (Appendix 4, Figures S5 and S6). The climatic positions calculated using CRU Time-series data (instead of WorldClim climate maps) to estimate species' climatic limits were strongly correlated to the climatic positions used in the final model ($r > 0.9$), and the results of the models run using

these climatic position estimates were very similar to those above (Appendix 4, Table S7, Figures S7 and S8). We were able to calculate climatic positions using GBIF occurrence data (instead of species' distribution maps) for 324 of the species found in our final dataset (6,681 populations), and these were also strongly correlated to the climatic positions reported here ($r > 0.78$; Appendix 4, Table S7). The overall patterns of results using climatic positions derived from GBIF data (with either WorldClim or CRU Time-series climate data) were on the whole similar to the results reported above (Appendix 4, Figures S9–S12). The key differences included that, unlike above, negative rates of population change were observed for populations (a) in agriculture where thermal extremes had got warmer and populations had high starting T_{\max} positions or high starting T_{\min} positions; Figures S10 and S12) and (b) in grasslands where populations had rapidly lost surrounding SNH and had low starting T_{\min} positions or low starting P_{\max} positions (Figure S9 and S11). Further, when GBIF data were used with WorldClim data to estimate climatic limits, other differences included (a) the negative rates of change observed above for populations in agriculture with lower starting P_{\min} positions under different rates of change in SNH and minimum precipitation (Figures 4d and 5d) were not observed (instead the rate of change varied around 0%–1% per year; Figures S9 and S10) and (b) the negative rates of change observed above for populations starting in grasslands with high P_{\max} positions and experiencing low negative rates of change in SNH (Figure 4c) were dampened to less negative rates of population change (between –1% and 0% per year; Figure S9).

Including the average annual rate of change in the percentage of SNH within a 1-km radius of each population, as in the model reported above, explained more variance (higher marginal R^2 values) than using rates of change within a 5-km radius. The model including the rate of change in SNH within a 10- or 50-km radius explained around the same amount of variance as within a 1-km radius, but as our hypotheses were focused on local climatic changes following land-use change, the 1-km radius was more appropriate. The model that included the average annual rate of change in the percentage of forest within a 1-km radius, rather than SNH, explained a very similar proportion of variation in the rate of population change and produced similar overall patterns to those observed above (although positive rates of change in grassland were often more extreme; Appendix 7, Figures S17 and S18). We also observed more negative rates of change for populations starting in agriculture with high T_{\max} positions when they experienced rapid increases in surrounding forest compared to SNH (Figure S17). We present the results of the model including SNH above, and that including rate of change in forest in the Supplementary information, due to our hypotheses focusing on the conversion of natural habitats (including both forest and grassland) to human-altered land uses.

Excluding populations whose time-series did not have a GAM $R^2 \geq 0.5$ removed around three-quarters of populations. The resulting model had a higher marginal R^2 and predicted more extreme rates of population change (in both the positive and negative direction) than those reported above, but patterns with respect to the environmental

variables discussed in the main findings above were similar (although a few differences in the pattern of the rate of change in population were observed for those starting within grassland, which may be due to the lower number ($n = 201$) of populations starting in grassland included in this model; Appendix 8, Figures S19–S21). Excluding time-series with $\bar{\lambda}_Y$ above and below the upper and lower 97.5th and 2.5th percentile, respectively, resulted in a model that explained slightly more variation (0.7%) than the final model, but overall patterns were similar (Appendix 9, Table S10, Figures S22–S24). Excluding species from the genus *Gyps* produced a model with a similar marginal R^2 value and very similar results to the model presented above (Appendix 10, Figures S25–S27). Running models without ectothermic species produced very similar results to those presented above, although rates of population change were shifted towards lower and more negative values (Appendix 11, Figures S28–S30). The models that excluded variables including the distance to range edge measure were very similar whether populations recorded outside of their species' ranges as stated by BirdLife International (2012) and IUCN (2016a, 2016b, 2017a, 2017b, 2017c, 2018a, 2018b, 2019a, 2019b, 2019c) were included or excluded (Appendix 12, Figures S31–S36). The majority of populations recorded outside of their species' ranges were relatively close to the range edge (70% were within 82km), with those further away generally being species invasive to the recorded location. Finally, cross-validation tests showed that there were no overly influential locations or species within our dataset (Appendix 13, Figures S37–S40).

4 | DISCUSSION

Vertebrate populations are not responding uniformly to land-use change across their distributions. Rather, we show that land-use change is interacting with climate change and climatic position to influence rates of population change. In particular, our results highlight the importance of taking a population's climatic position and the habitat they are within into account, as this led to large variation in the impact of the environmental changes we considered.

We show for the first time that a population's climatic position has an important influence on the rate of change in populations over time, in particular through its interactions with land-use type and environmental changes. Our results provided support for our first hypothesis regarding T_{\max} position: For populations initially in environments where maximum temperatures were closer to the species' hot thermal limit, those that were in agriculture and experienced more rapid losses in surrounding SNH (ie, high T_{\max} position + agriculture + SNH loss, Figure 4a) had more negative rates of population change compared to populations in forest or grassland. Again in line with our first hypothesis, we found that, within agriculture, for populations initially in environments with minimum temperatures close to their species' cold thermal limit, those that experienced increases in surrounding SNH (ie, low T_{\min} position + agriculture + SNH gain, Figure 4b) had positive rates of population change (whereas

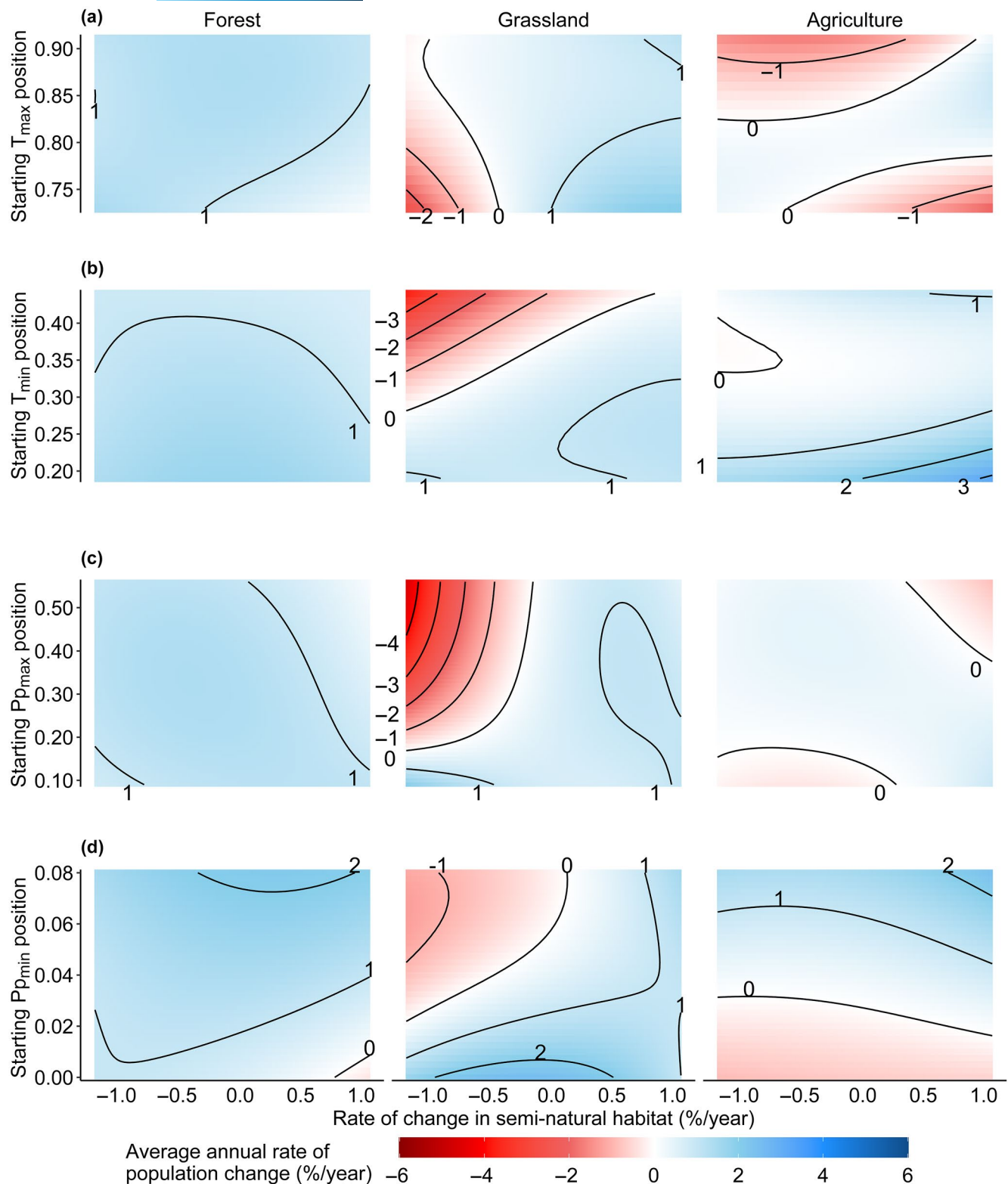
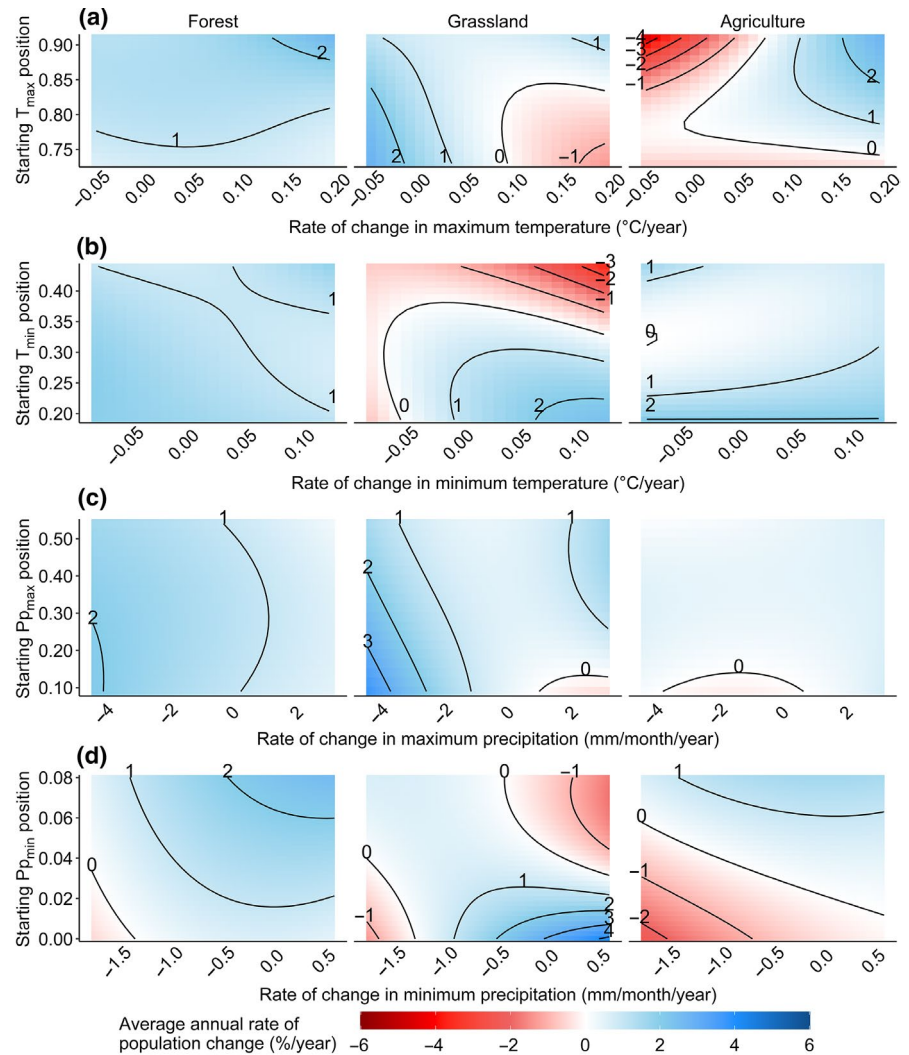


FIGURE 4 The average annual rate of population change across different starting land-use types, depending on: (i) the average annual rate of change in the percentage of semi-natural habitat within a 1-km radius; and (ii) a population's starting climatic position with regard to maximum temperature of the warmest month (T_{\max} , a), minimum temperature of the coldest month (T_{\min} , b), precipitation of the wettest month ($P_{p_{\max}}$, c) or precipitation of the driest month ($P_{p_{\min}}$, d). The x- and y-axes are truncated at the 10th and 90th percentile of sampled values of each variable. Contour lines (and labels) indicate changes in the average annual rate of population change [Colour figure can be viewed at [wileyonlinelibrary.com](https://onlinelibrary.wiley.com/doi/10.1111/gcb.15978)]

FIGURE 5 The average annual rate of population change across different starting land-use types, depending on: (i) the average annual rate of change in climate; and (ii) a population's starting climatic position. Climatic variables considered were maximum temperature of the warmest month (T_{\max} , a), minimum temperature of the coldest month (T_{\min} , b), precipitation of the wettest month (Pp_{\max} , c) and precipitation of the driest month (Pp_{\min} , d). The x- and y-axes are truncated at the 10th and 90th percentile of sampled values of each variable. Contour lines (and labels) indicate changes in the average annual rate of population change [Colour figure can be viewed at [wileyonlinelibrary.com](https://onlinelibrary.wiley.com)]



populations experiencing declines in SNH had lower rates of population change). These results highlight the need to, first, account for the population's climatic positions when investigating the impacts of land-use change (not just climate change) and second, include interactions occurring between drivers of change. These should be incorporated in both global biodiversity models, such as the one we present here, as well as local-scale conservation and management plans – these interactions and differences across species' ranges in responses to environmental changes cannot be overlooked if we are to mitigate the impact of anthropogenic changes on vertebrate populations around the world.

There were also unexpected results that were not in line with our hypotheses. For example, contrary to our second hypothesis, populations starting in agriculture that experienced rapid decreases in hot extremes had negative rates of population change, especially if they had high starting T_{\max} positions (ie, high T_{\max} position + agriculture + cooler hot extremes). Additionally, we observed that populations in agriculture, and initially in environments where maximum temperatures were further from the species' hot thermal limit, had more negative rates of population change in areas that had more rapid increases in surrounding SNH (ie, low T_{\max} position + agriculture + SNH gain). These observations may be due to individuals

recolonizing surrounding areas, which may have been restored (Nichols & Grant, 2007), and so moving out of agricultural areas. Whilst our analyses reveal several very important results, one limitation is that we are not able to determine *how* our focal variables are influencing population trends, whether it is through effects on birth, death, immigration or emigration rates. The mechanisms underlying how populations are influenced by climatic changes, and how their climatic positions may interact with the local climatic changes following land-use change are complex (Williams & Newbold, 2020). Further work is needed to explore the mechanisms underlying the influence of climatic position and interactions with land-use and climate change on population trends.

Regarding populations' precipitation positions, we found that our results using population time-series data contrasted in some respects when compared to a past space-for-time analysis (using data from the PREDICTS Project database; Williams & Newbold, 2021). The space-for-time analysis suggested that agricultural land uses had little impact on population abundance (relative to that in natural habitat) in environments where precipitation in the driest month was close to the species' dry limit (Williams & Newbold, 2021). However, here we observed that agricultural populations initially in environments where precipitation in the driest month

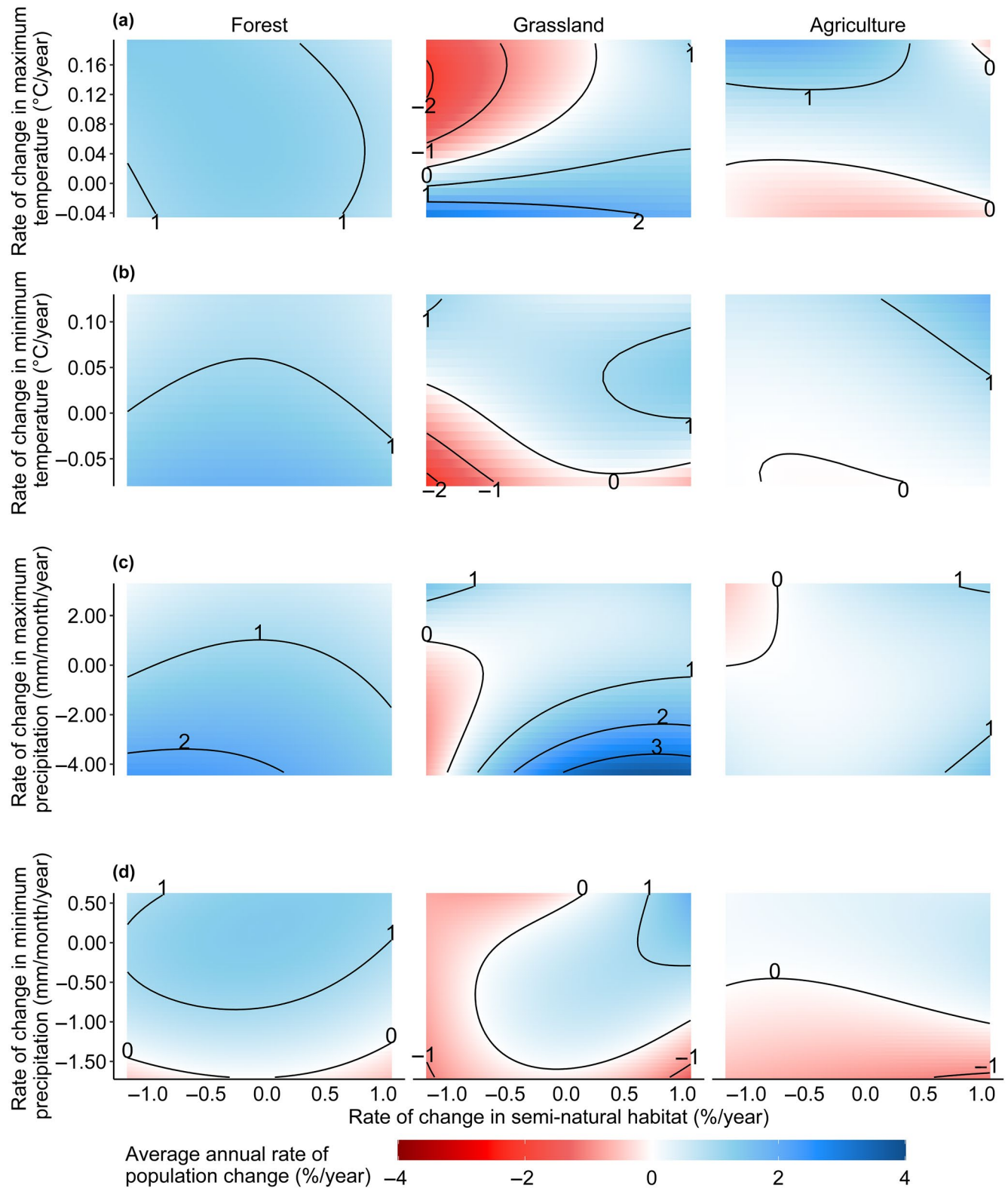


FIGURE 6 The average annual rate of population change across different starting land-use types, depending on: (i) the average annual rate of change in the percentage of semi-natural habitat within a 1-km radius; and (ii) average annual rate of change in climate with regard to maximum temperature of the warmest month (°C/year, a), minimum temperature of the coldest month (°C/year, b), precipitation of the wettest month (monthly mm/year, c) and precipitation of the driest month (monthly mm/year, d). The x- and y-axes are truncated at the 10th and 90th percentile of sampled values of each variable. Contour lines (and labels) indicate changes in the average annual rate of population change [Colour figure can be viewed at [wileyonlinelibrary.com](https://onlinelibrary.wiley.com)]

was closer to the species' dry limit (ie, low $P_{p_{min}}$ position + agriculture) had more negative rates of population change relative to populations in more natural habitats. The two types of analysis are capturing different attributes of population abundance (a snapshot in time vs. temporal trends), and resulting differences may be due to the influence of temporal lags, an interaction with global climate change or the locations of populations in the analyses. First, lags in responses to environmental changes (Lira et al., 2019) may mean that populations with lower $P_{p_{min}}$ positions are initially able to tolerate local changes towards drier conditions following land-use change, due to drought adaptations for example, but they may not be able to sustain numbers if the conditions continue. Lagged responses are not captured in most space-for-time analyses (De Palma et al., 2018). Second, ongoing drying trends in the tropics (Lau & Kim, 2015) may interact with precipitation position to lead to more rapid declines for populations with lower $P_{p_{min}}$ positions (indeed, we observe this in our results above, Figure 5d), a trend which may be hidden if the rate of climate change is not considered. Finally, and perhaps most importantly, most populations in our temporal analysis were found at temperate latitudes, and in the space-for-time analysis, the pattern regarding $P_{p_{min}}$ position was much stronger for agricultural populations at tropical latitudes (Williams & Newbold, 2021). This emphasizes the need to collect more time-series data for tropical populations (discussed further below), in order to explore geographic differences. Ultimately, exploring similar questions using both space-for-time and temporal analyses is key.

The land-use type a population was within when their population was first measured (starting land-use type: forest, grassland, agriculture, or other), and the percentage of surrounding SNH at the start of recording, also played vital roles within interactions. For example, we observe that, although populations starting in forests were generally increasing by around 1% per year, this rate was similar for populations with different starting climatic positions and experiencing different rates of land-use and climate change. This suggests that forests may act as buffers, providing climatic conditions and/or habitat quality (eg, due to the thermal buffering properties of a canopy layer and the complexity of microhabitats; De Frenne et al., 2019; González del Pliego et al., 2016) that protect populations from surrounding landscape-level (change in SNH) and global-level (climate change) environmental changes. Similarly, those populations surrounded by higher percentages of SNH at the start of recording generally had weaker and less negative population trends, suggesting that surrounding SNH can also help buffer populations from land-use and climatic changes, across different climatic positions. Conversely, we observed that variation in the rate of population change across different climatic positions and rates of land-use and climate change was often greater in grassland habitats compared to forest or agriculture. This suggests that grassland populations may be especially sensitive to environmental changes. The majority of grassland populations were birds, and it has previously been found that grassland birds respond more strongly than forest birds to climatic changes (Jarzyna et al., 2016). In addition, it

has been highlighted that many grassland bird species may be particularly sensitive to habitat loss due to being area-sensitive (Herkert, 1994; Vickery et al., 1994). Overall, this emphasizes that habitat type needs to be accounted for within large-scale models analysing the impacts of drivers of change across multiple land uses – otherwise, the weight of any driver's influence may be dampened or obscured due to the buffering effects of natural habitats.

By analysing time-series data from both the LPD and BioTIME database together, not only were we able to analyse over 7,000 vertebrate populations, but we could also highlight some of the differences between the databases, which may contribute to the conflicting results between previous studies analysing these databases separately (eg, Dornelas et al., 2019; WWF 2020). After filtering, there were roughly the same number of populations from tropical ($n = 174$) and temperate ($n = 193$) latitudes from the LPD, whereas all BioTIME populations ($n = 6,756$) came from temperate latitudes. Even though abiotic factors are suggested to have a greater impact on species distributions at higher latitudes (Khaliq et al., 2017; MacArthur, 1972), the tropics have continuously been identified as particularly vulnerable to drivers of change such as land-use and climate change (Brook et al., 2008; Newbold et al., 2020). Further, previous global studies examining the impact of local climatic changes following land-use change have found greater differences in communities between natural and human-altered land uses in tropical than temperate latitudes (Williams et al., 2020). Reasons for this include the relative stability (past and present) of the tropical climate (Janzen, 1967; Pacifici et al., 2017), the smaller average range sizes of species within the tropics (Stevens, 1989; Thuiller et al., 2005), the fact that tropical species are often living closer to their maximum thermal tolerance limits (Deutsch et al., 2008; Sunday et al., 2014), and the larger proportion of specialist species (habitat and dietary specialists) inhabiting the tropics (Forister et al., 2015). Consequently, the skew of BioTIME data towards temperate assemblages may not give an accurate representation of global population trends. Indeed, analyses of vertebrate populations of forest specialists from the LPD found that the average abundance trends were positive in temperate biomes and negative in tropical biomes (Green et al., 2020). Ideally, we would test whether population trends were influenced differently by our focal variables depending on whether the population was at a tropical or temperate latitude. However, there were insufficient tropical data to do so. In our final dataset, the LPD contributed populations from 42 countries, whereas the BioTIME database contributed populations from just 4 countries (the United States of America, Canada, South Africa and Brazil; Appendix 2, Figure S1). Historical pressures on biodiversity can impact vulnerability to present-day environmental changes (Balmford, 1996). Therefore, analyses based on data from a small number of countries need to take this into account and, in the case of the BioTIME database, the countries contributing data all have long histories of environmental changes (although, in the case of Brazil, this varies spatially within the country; Goldewijk, 2001; Goldewijk et al., 2011; Nehren et al., 2013). Consequently, this

may be another reason for disparities between previous studies using data from the LPD versus BioTIME database.

Using species' distribution maps and climate data from WorldClim to estimate species' realized climatic tolerance limits meant that we were not able to take into account climatic adaptations over time, intraspecific differences in climatic tolerances, or microclimatic conditions. In addition, despite excluding migratory species from our dataset, populations may still utilize different local habitats (eg, different microhabitats or move across local-scale elevations) throughout the year. However, at present, the data are not available to include/account for these variables, especially for the large number of populations (over 7,000 populations, covering almost 350 species) that were included in this analysis. Hopefully, it will be possible to account for these variables in future. Further, we use estimates of realized climatic tolerance limits, which can be influenced by factors other than climate, such as dispersal barriers and biotic interactions (HilleRisLambers et al., 2013; Peterson et al., 2011). Nevertheless, we use these rather than physiological climatic tolerance limits because physiological data are available for very few species, the metrics produced in laboratory tests are often incomparable to one another (due to different measurement procedures), and laboratory tests have been criticized for not being reflective of real-world conditions (Araújo et al., 2013; Rezende et al., 2014; Sunday et al., 2012).

In conclusion, local land-use changes and global climate changes are interacting to impact vertebrate population trends around the world. Further, these interactions do not impact populations uniformly across species' ranges. Rather, a population's climatic position is key within these interactions and can lead to the impacts of land-use and climatic changes being intensified or dampened, especially within grassland and agricultural land uses. Consequently, we highlight the importance of taking a population's climatic position into account, not just when studying the impacts of climate change (Soroye et al., 2020), but also land-use change. Even though the effects of these interactions are complex, and further work is needed on the mechanisms underlying how these variables influence populations, our results allow us to identify populations that may be at more risk of decline. For example, our results highlight that populations in agricultural land uses where maximum temperatures were closer to their hot thermal limit, declined at faster rates when there had also been rapid losses in surrounding semi-natural habitats. In order to prevent further population declines and mitigate the impact of anthropogenic changes, we cannot ignore interactions between drivers of change, and we must account for variation across species' ranges in responses to local and global environmental changes in both local conservation strategies and global models.

ACKNOWLEDGEMENTS

We would like to thank Louise McRae for her invaluable help with the Living Planet database, Stuart Butchart and BirdLife International for providing BirdLife data and range maps, and Geoff Griffiths, Syed Amir Manzoor and Christine Howard for

useful discussion regarding the ESA CCI land-cover data and ways of grouping the classes. This work was supported by a Royal Society Research Grant to TN, which supported the PhD studentship of JJW (RG160501), a Royal Society University Research Fellowship to TN (UF150526), and a Royal Society International Exchanges Grant to TN (IE161031).

CONFLICT OF INTEREST

The authors declare no competing interests.

DATA AVAILABILITY STATEMENT

Data and code are available in a figshare repository (<https://doi.org/10.6084/m9.figshare.16895851>; for data classified as confidential by the Living Planet Index database, species' names are hidden). The full BioTIME database can be downloaded from <http://bioti.me.st-andrews.ac.uk/downloadArea.php> and the Living Planet Index database (apart from the confidential data) can be found at https://livingplanetindex.org/data_portal. The European Space Agency Climate Change Initiative land cover maps can be downloaded from <https://catalogue.ceda.ac.uk/uuid/b382ebe6679d44b8b0e68ea4ef4b701c>. The Climatic Research Unit Time-series data v. 4.03 can be downloaded from <https://catalogue.ceda.ac.uk/uuid/10d3e3640f004c578403419aac167d82>. The WorldClim Version 1.4 climatic variable maps can be downloaded from <http://www.worldclim.com/version1> and species distribution maps can be downloaded or requested from <https://www.iucnredlist.org/resources/spatial-data-download> and <http://datazone.birdlife.org/species/requestdis>, respectively.

ORCID

Jessica J. Williams  <https://orcid.org/0000-0002-8275-7597>

Fiona Spooner  <https://orcid.org/0000-0001-6640-8621>

Tim Newbold  <https://orcid.org/0000-0001-7361-0051>

REFERENCES

- Allan, J. R., Watson, J. E. M., Di Marco, M., O'Bryan, C. J., Possingham, H. P., Atkinson, S. C., & Venter, O. (2019). Hotspots of human impact on threatened terrestrial vertebrates. *PloS Biology*, 17(3), e3000158. <https://doi.org/10.1371/journal.pbio.3000158>
- Antão, L. H., Bates, A. E., Blowes, S. A., Waldock, C., Supp, S. R., Magurran, A. E., Dornelas, M., & Schipper, A. M. (2020). Temperature-related biodiversity change across temperate marine and terrestrial systems. *Nature Ecology and Evolution*, 4(7), 927–933. <https://doi.org/10.1038/s41559-020-1185-7>
- Araújo, M. B., Ferri-Yáñez, F., Bozinovic, F., Marquet, P. A., Valladares, F., & Chown, S. L. (2013). Heat freezes niche evolution. *Ecology Letters*, 16(9), 1206–1219. <https://doi.org/10.1111/ele.12155>
- Balmford, A. (1996). Extinction filters and current resilience: The significance of past selection pressures for conservation biology. *Trends in Ecology and Evolution*, 11(5), 193–196. [https://doi.org/10.1016/0169-5347\(96\)10026-4](https://doi.org/10.1016/0169-5347(96)10026-4)
- Barton, K. (2020). MuMIn: Multi-model inference. *R Package Version*, 1(43), 17. <https://CRAN.R-project.org/package=MuMIn>
- Bates, D., Maechler, M., Bolker, B., & Walker, S. (2015). Fitting linear mixed-effects models using lme4. *Journal of Statistical Software*, 67(1), 1–48. <https://doi.org/10.18637/jss.v067.i01>

- BirdLife International. (2018). BirdLife International data zone. BirdLife International, Cambridge, UK. www.datazone.birdlife.org/home. Accessed November 2018.
- BirdLife International, NatureServe. (2012). Bird species distribution maps of the world. Version, 2.0. <http://www.birdlife.org/datazone/info/spcdownload>
- Brook, B. W., Sodhi, N. S., & Bradshaw, C. J. A. (2008). Synergies among extinction drivers under global change. *Trends in Ecology and Evolution*, 23(8), 453–460. <https://doi.org/10.1016/j.tree.2008.03.011>
- Collen, B., Loh, J., Whitmee, S., McRae, L., Amin, R., & Baillie, J. E. M. (2009). Monitoring change in vertebrate abundance: the living planet index. *Conservation Biology*, 23(2), 317–327. <https://doi.org/10.1111/j.1523-1739.2008.01117.x>
- Daskalova, G. N., Myers-Smith, I. H., Bjorkman, A. D., Blowes, S. A., Supp, S. R., Magurran, A. E., & Dornelas, M. (2020). Landscape-scale forest loss as a catalyst of population and biodiversity change. *Science*, 368(6497), 1341–1347. <https://doi.org/10.1126/science.aba1289>
- De Frenne, P., Zellweger, F., Rodríguez-Sánchez, F., Scheffers, B. R., Hylander, K., Luoto, M., Vellend, M., Verheyen, K., & Lenoir, J. (2019). Global buffering of temperatures under forest canopies. *Nature Ecology & Evolution*, 3, 744–749. <https://doi.org/10.1038/s41559-019-0842-1>
- De Palma, A., Sanchez-Ortiz, K., Martin, P. A., Chadwick, A., Gilbert, G., Bates, A. E., Börger, L., Contu, S., & Hill, S. & Purvis, A. (2018). Challenges with inferring how land-use affects terrestrial biodiversity: Study design, time, space and synthesis. *Advances in Ecological Research*, 58(February), 163–199. <https://doi.org/10.1016/bs.aecr.2017.12.004>
- Defourny, P., Bontemps, S., Lamarche, C., Brockmann, C., Boettcher, M., Wevers, J., & Kirches, G. (2017). Land Cover CCI: Product User Guide Version 2.0. Available at: <https://maps.elie.ucl.ac.be/CCI/viewer/>
- Deutsch, C. A., Tewksbury, J. J., Huey, R. B., Sheldon, K. S., Ghalambor, C. K., Haak, D. C., & Martin, P. R. (2008). Impacts of climate warming on terrestrial ectotherms across latitude. *Proceedings of the National Academy of Sciences*, 105(18), 6668–6672. <https://doi.org/10.1073/pnas.0709472105>
- Dornelas, M., Antão, L. H., Moyes, F., Bates, A. E., Magurran, A. E., Adam, D., Akhmetzhanova, A. A., Appeltans, W., Arcos, J. M., Arnold, H., Ayyappan, N., Badihi, G., Baird, A. H., Barbosa, M., Barreto, T. E., Bässler, C., Bellgrove, A., Belmaker, J., Benedetti-Cecchi, L., ... Hickler, T. (2018). BioTIME: A database of biodiversity time series for the Anthropocene. *Global Ecology and Biogeography*, 27(7), 760–786. <https://doi.org/10.1111/geb.12729>
- Dornelas, M., Gotelli, N. J., Shimadzu, H., Moyes, F., Magurran, A. E., & McGill, B. J. (2019). A balance of winners and losers in the Anthropocene. *Ecology Letters*, 22(5), 847–854. <https://doi.org/10.1111/ele.13242>
- ESRI. (2015). ArcGIS Desktop: Version. 10.4. Environmental Systems Research Institute.
- Forister, M. L., Novotny, V., Panorska, A. K., Baje, L., Basset, Y., Butterill, P. T., Cizek, L., Coley, P. D., Dem, F., Diniz, I. R., Drozd, P., Fox, M., Glassmire, A. E., Hazen, R., Hrcek, J., Jahner, J. P., Kaman, O., Kozubowski, T. J., Kursar, T. A., ... Dyer, L. A. (2015). The global distribution of diet breadth in insect herbivores. *Proceedings of the National Academy of Sciences of the United States of America*, 112(2), 442–447. <https://doi.org/10.1073/pnas.1423042112>
- Frishkoff, L. O., Hadly, E. A., & Daily, G. C. (2015). Thermal niche predicts tolerance to habitat conversion in tropical amphibians and reptiles. *Global Change Biology*, 21(11), 3901–3916. <https://doi.org/10.1111/gcb.13016>
- Frishkoff, L. O., Karp, D. S., Flanders, J. R., Zook, J., Hadly, E. A., Daily, G. C., & M'Gonigle, L. K. (2016). Climate change and habitat conversion favour the same species. *Ecology Letters*, <https://doi.org/10.1111/ele.12645>
- GBIF.org. (2015). GBIF Occurrence Download. <https://doi.org/10.15468/dl.rllzli>
- Gnanadesikan, G. E., Pearse, W. D., & Shaw, A. K. (2017). Evolution of mammalian migrations for refuge, breeding, and food. *Ecology and Evolution*, 7(15), 5891–5900. <https://doi.org/10.1002/ece3.3120>
- Goldewijk, K. K. (2001). Estimating global land use change over the past 300 years: The HYDE database. *Global Biogeochemical Cycles*, 15(2), 417–433. <https://doi.org/10.1029/1999GB001232>
- Goldewijk, K. K., Beusen, A., Van Drecht, G., & De Vos, M. (2011). The HYDE 3.1 spatially explicit database of human-induced global land-use change over the past 12,000 years. *Global Ecology and Biogeography*, 20(1), 73–86. <https://doi.org/10.1111/j.1466-8238.2010.00587.x>
- Gonzalez, A., Cardinale, B. J., Allington, G. R. H., Byrnes, J., Arthur Endsley, K., Brown, D. G., Hooper, D. U., Isbell, F., O'Connor, M. I., & Loreau, M. (2016). Estimating local biodiversity change: A critique of papers claiming no net loss of local diversity. *Ecology*, 97(8), 1949–1960. <https://doi.org/10.1890/15-1759.1>
- González del Pliego, P., Scheffers, B. R., Basham, E. W., Woodcock, P., Wheeler, C., Gilroy, J. J., Medina Uribe, C. A., Haugaasen, T., Freckleton, R. P., & Edwards, D. P. (2016). Thermally buffered microhabitats recovery in tropical secondary forests following land abandonment. *Biological Conservation*, 201(September), 385–395. <https://doi.org/10.1016/j.biocon.2016.07.038>
- Green, E. J., McRae, L., Freeman, R., Harfoot, M. B. J., Hill, S. L. L., Baldwin-Cantello, W., & Simonson, W. D. (2020). Below the canopy: global trends in forest vertebrate populations and their drivers. *Proceedings of the Royal Society B: Biological Sciences*, 287(1928), 20200533. <https://doi.org/10.1098/rspb.2020.0533>
- Harris, I. C. & Jones, P. D. (2020). CRU TS4.03: Climatic Research Unit (CRU) Time-Series (TS) version 4.03 of high-resolution gridded data of month-by-month variation in climate (Jan. 1901– Dec. 2018). Centre for Environmental Data Analysis, downloaded on 22 January 2020. <https://doi.org/10.5285/10d3e364f004c578403419aac167d82>
- Herkert, J. R. (1994). The effects of habitat fragmentation on midwestern grassland bird communities. *Ecological Applications*, 4(3), 461–471. <https://doi.org/10.2307/1941950>
- Herk, K. M. B., Skidmore, A. K., & Fahr, J. (2017). Macroecological conclusions based on IUCN expert maps: A call for caution. *Global Ecology and Biogeography*, 26(8), 930–941. <https://doi.org/10.1111/geb.12601>
- Hijmans, R. J. (2019). *raster: Geographic data analysis and modeling. R package version 2.8-19*. <https://CRAN.R-project.org/package=raster>
- Hijmans, R. J., Cameron, S. E., Parra, J. L., Jones, P. G., & Jarvis, A. (2005). Very high resolution interpolated climate surfaces for global land areas. *International Journal of Climatology*, 25(15), 1965–1978. <https://doi.org/10.1002/joc.1276>
- HilleRisLambers, J., Harsch, M. A., Ettinger, A. K., Ford, K. R., & Theobald, E. J. (2013). How will biotic interactions influence climate change-induced range shifts? *Annals of the New York Academy of Sciences*, 1297, 112–125. <https://doi.org/10.1111/nyas.12182>
- Hurlbert, A. H., & Jetz, W. (2007). Species richness, hotspots, and the scale dependence of range maps in ecology and conservation. *Proceedings of the National Academy of Sciences*, 104(33), 13384–13389. <https://doi.org/10.1073/pnas.0704469104>
- IPBES. *Global assessment report on biodiversity and ecosystem services of the Intergovernmental Science-Policy Platform on Biodiversity and Ecosystem Services*. (2019). In E. S. Brondizio, J. Settele, S. Díaz, & H. T. Ngo (Eds.). IPBES secretariat.
- IUCN. (2016a). The IUCN Red List of Threatened Species. Version 2016-1. <http://www.iucnredlist.org>
- IUCN. (2016b). The IUCN Red List of Threatened Species. Version 2016-3. <http://www.iucnredlist.org>
- IUCN. (2017a). The IUCN Red List of Threatened Species. Versions, 2017-1, 2017-2, 2017-3. <http://www.iucnredlist.org>

- IUCN. (2017b). The IUCN Red List of Threatened Species. Version 2017-2. <http://www.iucnredlist.org>
- IUCN. (2017c). The IUCN Red List of Threatened Species. Version 2017-3. <http://www.iucnredlist.org>
- IUCN. (2018a). The IUCN Red List of Threatened Species. Version 2018-1. <http://www.iucnredlist.org>
- IUCN. (2018b). The IUCN Red List of Threatened Species. Version 2018-2. <http://www.iucnredlist.org>
- IUCN. (2019a). The IUCN Red List of Threatened Species. Version 2019-1. <http://www.iucnredlist.org>
- IUCN. (2019b). The IUCN Red List of Threatened Species. Version 2019-2. <http://www.iucnredlist.org>
- IUCN. (2019c). The IUCN Red List of Threatened Species. Version 2019-3. <http://www.iucnredlist.org>
- Janzen, D. H. (1967). Why mountain passes are higher in the tropics. *The American Naturalist*, 101, 233–249. <https://doi.org/10.1086/282487>
- Jarzyna, M. A., Zuckerberg, B., Finley, A. O., & Porter, W. F. (2016). Synergistic effects of climate and land cover: grassland birds are more vulnerable to climate change. *Landscape Ecology*, 31, 2275–2290. <https://doi.org/10.1007/s10980-016-0399-1>
- Jung, M., Dahal, P. R., Butchart, S. H. M., Donald, P. F., Lamo, X. D., Lesiv, M., & Visconti, P. (2020). A global map of terrestrial habitat types. *Scientific Data*, 1–8. <https://doi.org/10.1038/s41597-020-00599-8>
- Karp, D. S., Frishkoff, L. O., Echeverri, A., Zook, J., Juárez, P., & Chan, K. M. A. (2017). Agriculture erases climate-driven β -diversity in Neotropical bird communities. *Global Change Biology*, 24(1), 338–349. <https://doi.org/10.1111/gcb.13821>
- Khalik, I., Böhning-Gaese, K., Prinzinger, R., Pfenninger, M., & Hof, C. (2017). The influence of thermal tolerances on geographical ranges of endotherms. *Global Ecology and Biogeography*, 26(6), 650–668. <https://doi.org/10.1111/geb.12575>
- ESA Land Cover and CCI project team, Defourny, P. (2019). ESA Land Cover Climate Change Initiative (Land_Cover_cci): Global Land Cover Maps, Version 2.0.7. Centre for Environmental Data Analysis. downloaded on 28 January 2020. <https://catalogue.ceda.ac.uk/uuid/b382ebe6679d44b8b0e68ea4ef4b701c>
- Lau, W. K. M., & Kim, K. M. (2015). Robust Hadley circulation changes and increasing global dryness due to CO₂ warming from CMIP5 model projections. *Proceedings of the National Academy of Sciences of the United States of America*, 112(12), 3630–3635. <https://doi.org/10.1073/pnas.1418682112>
- Le Provost, G., Badenhausser, I., Le Bagousse-Pinguet, Y., Clough, Y., Henckel, L., Violle, C., Bretagnolle, V., Roncoroni, M., & Manning, P. (2020). Land-use history impacts functional diversity across multiple trophic groups. *Proceedings of the National Academy of Sciences of the United States of America*, 117(3), 1573–1579. <https://doi.org/10.1073/pnas.1910023117>
- Leung, B., Hargreaves, A. L., Greenberg, D. A., McGill, B., Dornelas, M., & Freeman, R. (2020). Clustered versus catastrophic global vertebrate declines. *Nature*, 588(7837), 267–271. <https://doi.org/10.1038/s41586-020-2920-6>
- Liebl, A. L., & Martin, L. B. (2012). Exploratory behaviour and stressor hyper responsiveness facilitate range expansion of an introduced songbird. *Proceedings of the Royal Society B: Biological Sciences*, 279(1746), 4375–4381. <https://doi.org/10.1098/rspb.2012.1606>
- Lira, P. K., de Souza Leite, M., & Metzger, J. P. (2019). Temporal lag in ecological responses to landscape change: Where are we now? *Current Landscape Ecology Reports*, 4(3), 70–82. <https://doi.org/10.1007/s40823-019-00040-w>
- Living Planet Index database. (2020). www.livingplanetindex.org/. Downloaded January 2020.
- MacArthur, R. H. (1972). *Geographical ecology: Patterns in the distribution of species*. Harper and Row.
- Mantyka-Pringle, C., Martin, T. G., & Rhodes, J. R. (2012). Interactions between climate and habitat loss effects on biodiversity: A systematic review and meta-analysis. *Global Change Biology*, 18(4), 1239–1252. <https://doi.org/10.1111/j.1365-2486.2011.02593.x>
- Nakagawa, S., & Schielzeth, H. (2013). A general and simple method for obtaining R² from generalized linear mixed-effects models. *Methods in Ecology and Evolution*, 4(2), 133–142. <https://doi.org/10.1111/j.2041-210x.2012.00261.x>
- Nehren, U., Kirchner, A., Sattler, D., Turetta, A. P., & Heinrich, J. (2013). Impact of natural climate change and historical land use on landscape development in the Atlantic Forest of Rio de Janeiro, Brazil. *Anais Da Academia Brasileira De Ciencias*, 85(2), 497–518. <https://doi.org/10.1590/S0001-37652013000200004>
- Newbold, T., Oppenheimer, P., Etard, A., & Williams, J. J. (2020). Tropical and Mediterranean biodiversity is disproportionately sensitive to land-use and climate change. *Nature Ecology & Evolution*, 4, 1630–1638. <https://doi.org/10.1038/s41559-020-01303-0>
- Nichols, O. G., & Grant, C. D. (2007). Vertebrate fauna recolonization of restored bauxite mines - Key findings from almost 30 years of monitoring and research. *Restoration Ecology*, 15(SUPPL. 4), 116–126. <https://doi.org/10.1111/j.1526-100X.2007.00299.x>
- Northrup, J. M., Rivers, J. W., Yang, Z., & Betts, M. G. (2019). Synergistic effects of climate and land-use change influence broad-scale avian population declines. *Global Change Biology*, 25(5), 1561–1575. <https://doi.org/10.1111/gcb.14571>
- Nowakowski, A. J., Watling, J. I., Whitfield, S. M., Todd, B. D., Kurz, D. J., & Donnelly, M. A. (2017). Tropical amphibians in shifting thermal landscapes under land-use and climate change. *Conservation Biology*, 31(1), 96–105. <https://doi.org/10.1111/cobi.12769>
- Oliver, T. H., & Morecroft, M. D. (2014). Interactions between climate change and land use change on biodiversity: attribution problems, risks, and opportunities. *Wiley Interdisciplinary Reviews: Climate Change*, 5(3), 317–335. <https://doi.org/10.1002/wcc.271>
- Orme, C. D. L., Mayor, S., Anjos, L., Develey, P. F., Hatfield, J. H., Morante-filho, J. C., & Banks-leite, C. (2019). Distance to range edge determines sensitivity to deforestation. *Nature Ecology & Evolution*, 3(June), 886–891. <https://doi.org/10.1038/s41559-019-0889-z>
- Pacifici, M., Visconti, P., Butchart, S. H. M., Watson, J. E. M., Cassola, F. M., & Rondinini, C. (2017). Species' traits influenced their response to recent climate change. *Nature Climate Change*, 7(3), 205–208. <https://doi.org/10.1038/nclimate3223>
- Peterson, A. T., Soberón, J., Pearson, R. G., Anderson, R. P., Martinez-Meyer, E., Nakamura, M., & Araújo, M. B. (2011). *Ecological niches and geographic distributions*. Princeton University Press.
- Pierce, D. (2019). ncd4: Interface to Unidata netCDF (Version 4 or Earlier) Format Data Files. R Package Version 1.17. <https://CRAN.R-project.org/package=ncdf4>
- R Core Team. (2019). *R: A language and environment for statistical computing*. R Foundation for Statistical Computing. <https://www.R-project.org/>
- Rezende, E. L., Castañeda, L. E., & Santos, M. (2014). Tolerance landscapes in thermal ecology. *Functional Ecology*, 28(4), 799–809. <https://doi.org/10.1111/1365-2435.12268>
- Senior, R. A., Hill, J. K., Benedick, S., & Edwards, D. P. (2017). Tropical forests are thermally buffered despite intensive selective logging. *Global Change Biology*, 24(3), 1267–1278. <https://doi.org/10.1111/gcb.13914>
- Shackelford, G. E., Steward, P. R., German, R. N., Sait, S. M., & Benton, T. G. (2015). Conservation planning in agricultural landscapes: Hotspots of conflict between agriculture and nature. *Diversity and Distributions*, 21(3), 357–367. <https://doi.org/10.1111/ddi.12291>
- Sirami, C., Caplat, P., Popy, S., Clamens, A., Arlettaz, R., Jiguet, F., & Martin, J. L. (2017). Impacts of global change on species distributions: obstacles and solutions to integrate climate and land use. *Global Ecology and Biogeography*, 26(4), 385–394. <https://doi.org/10.1111/geb.12555>

- Soroye, P., Newbold, T., & Kerr, J. (2020). Climate change contributes to widespread declines among bumble bees across continents. *Science*, 367(6478), 685–688. <https://doi.org/10.1126/science.aax8591>
- Spooner, F. E. B., Pearson, R. G., & Freeman, R. (2018). Rapid warming is associated with population decline among terrestrial birds and mammals globally. *Global Change Biology*, 24(10), 4521–4531. <https://doi.org/10.1111/gcb.14361>
- Srinivasan, U., Elsen, P. R., & Wilcove, D. S. (2019). Annual temperature variation influences the vulnerability of montane bird communities to land-use change. *Ecography*, 42, 1–11. <https://doi.org/10.1111/ecog.04611>
- Stevens, G. C. (1989). The latitudinal gradient in geographical range: How so many species coexist in the tropics. *The American Naturalist*, 133(2), 240–256.
- Sunday, J. M., Bates, A. E., & Dulvy, N. K. (2012). Thermal tolerance and the global redistribution of animals. *Nature Climate Change*, 2(9), 686–690. <https://doi.org/10.1038/nclimate1539>
- Sunday, J. M., Bates, A. E., Kearney, M. R., Colwell, R. K., Dulvy, N. K., Longino, J. T., & Huey, R. B. (2014). Thermal-safety margins and the necessity of thermoregulatory behavior across latitude and elevation. *Proceedings of the National Academy of Sciences of the United States of America*, 111(15), 5610–5615. <https://doi.org/10.1073/pnas.1316145111>
- Thuiller, W., Lavorel, S., & Araújo, M. B. (2005). Niche properties and geographical extent as predictors of species sensitivity to climate change. *Global Ecology and Biogeography*, 14, 347–357. <https://doi.org/10.1111/j.1466-822x.2005.00162.x>
- Vickery, P. D., Hunter, M. L. Jr, & Melvin, S. M. (1994). Effects of habitat area on the distribution of grassland birds in Maine. *Conservation Biology*, 8(4), 1087–1097. <https://doi.org/10.1046/j.1523-1739.1994.08041087.x>
- Waldock, C. A., De Palma, A., Borges, P. A. V., & Purvis, A. (2020). Insect occurrence in agricultural land-uses depends on realized niche and geographic range properties. *Ecography*, 1–12. <https://doi.org/10.1111/ecog.05162>
- Wickham, H. (2011). The split-apply-combine strategy for data analysis. *Journal of Statistical Software*, 40(1), 1–29. <http://www.jstatsoft.org/v40/i01/>
- Wickham, H., François, R., Henry, L., & Müller, K. (2019). dplyr: A grammar of data manipulation. R Package Version 0.8.3. <https://CRAN.R-project.org/package=dplyr>
- Wickham, H., & Henry, L. (2019). tidyr: Tidy Messy Data. R Package Version 1.0.0. <https://CRAN.R-project.org/package=tidyr>
- Williams, J. J., Bates, A. E., & Newbold, T. (2020). Human-dominated land uses favour species affiliated with more extreme climates, especially in the tropics. *Ecography*, 43, 391–405. <https://doi.org/10.1111/ecog.04806>
- Williams, J. J., Freeman, R., Spooner, F., & Newbold, T. (2021). Data and code from: Vertebrate population trends are influenced by interactions between land use, climatic position, habitat loss and climate change. figshare. Dataset. <https://doi.org/10.6084/m9.figshare.16895851.v1>
- Williams, J. J., & Newbold, T. (2020). Local climatic changes affect biodiversity responses to land use: A review. *Diversity and Distributions*, 26(1), 76–92. <https://doi.org/10.1111/ddi.12999>
- Williams, J. J., & Newbold, T. (2021). Vertebrate responses to human land use are influenced by their proximity to climatic tolerance limits. *Diversity and Distributions*, 27(7), 1308–1323. <https://doi.org/10.1111/ddi.13282>
- WWF. (2020). *Living Planet Report 2020 - Bending the curve of biodiversity loss*. R. E. A. Almond, M. Grooten, & T. Petersen (Eds). WWF.

SUPPORTING INFORMATION

Additional supporting information may be found in the online version of the article at the publisher's website.

How to cite this article: Williams, J. J., Freeman, R., Spooner, F., & Newbold, T. (2022). Vertebrate population trends are influenced by interactions between land use, climatic position, habitat loss and climate change. *Global Change Biology*, 28, 797–815. <https://doi.org/10.1111/gcb.15978>